

Heavy-meson hadroproduction: open issues

M.V. Garzelli*

*Dipartimento di Fisica e Astronomia, Università degli Studi di Firenze & INFN, Firenze,
Institut für Theoretische Physik, Eberhard Karls Universität Tübingen,
E-mail: maria.vittoria.garzelli@cern.ch*

S. Alekhin

*II Institut für Theoretische Physik, Universität Hamburg,
E-mail: sergey.alekhin@desy.de*

M. Benzke

*II Institut für Theoretische Physik, Universität Hamburg,
E-mail: michael.benzke@desy.de*

B. Kniehl

*II Institut für Theoretische Physik, Universität Hamburg,
E-mail: bernd.kniehl@desy.de*

S.-O. Moch

*II Institut für Theoretische Physik, Universität Hamburg,
E-mail: sven-olaf.moch@desy.de*

O. Zenaiev

*CERN, Experimental Physics Department, Geneva, E-mail:
oleksandr.zenaiev@cern.ch*

We discuss open issues in the description of single-inclusive open heavy-meson production in pp and pA collisions, considering different flavour-number schemes. Solving these issues is important for improving the accuracy of PDF fits and of predictions in high-energy astroparticle physics.

*14th International Symposium on Radiative Corrections (RADCOR2019)
9-13 September 2019
Palais des Papes, Avignon, France*

*Speaker.

1. Introduction

Heavy mesons and baryons include at least one heavy quark $Q = (c, b)$ as valence quark in their composition [1]. The masses of these quarks are large with respect to Λ_{QCD} , but much smaller than the typical center-of-mass energies \sqrt{s} reached at the Tevatron and the Large Hadron Collider (LHC). In pp and $p\bar{p}$ interactions, these quarks can be produced in perturbative QCD either during a hard-scattering process or as a result of a $g \rightarrow Q\bar{Q}$ splitting during the initial or final state radiation processes. An intrinsic heavy-quark component in the proton is also advocated by the theoretical considerations in Ref. [2], but the experimental results obtained so far at accelerators do not hint at a large contribution of this kind. After the evolution to low scales, heavy quarks combine with other partons, giving rise to heavy hadrons. The production of heavy hadrons can be described in different flavour-number schemes, according to the adopted values for the masses of the heavy quarks.

2. Benefits and shortcomings of different flavour number schemes for single-inclusive heavy-hadron production at hadronic colliders

When using a fixed-flavour-number scheme (FFNS), with a constant number of active light flavours n_l at all scales, the mass of the heavy quark is kept different from zero in all parts of the computation. The partonic hard scattering is initiated by the light flavours, the heavy-quark parton distribution function (PDF) vanishing at all scales. The evolution of the renormalized strong coupling constant $\alpha_S^{(n_l)}$ and the $\alpha_S^{(n_l)}(m_Z^2)$ value are consistent with the adopted PDF fit. This approach preserves contributions proportional to powers of m_Q/p_T , where p_T is the transverse momentum of the emitted quark, but does not resum logarithms of (p_T/m_Q) , which might become large if $p_T \gg m_Q$. The transition from heavy quarks to heavy hadrons is described by phenomenological fragmentation functions (FF).

When using the zero-mass variable-flavour-number scheme (ZM-VFNS), the masses of the heavy quarks (c, b, t) are neglected and the number of active flavours in the PDFs increases from 3 to 4 to 5 to 6 with an increasing factorization scale μ , when crossing the μ_c, μ_b and μ_t matching scales, respectively. These matching scales often coincide with the corresponding heavy-quark mass values m_c, m_b, m_t , but can also be kept larger, i.e. $\mu_Q \geq m_Q$ [3]. The number of active flavours in the β function governing the α_S evolution with renormalization scale is chosen consistently. This approach does not preserve the terms proportional to powers of m_Q/p_T , which would be important to include when the characteristic scale of the hard-scattering process is not too large with respect to m_Q . On the other hand, a rigorous factorization theorem can be written which allows to effectively resum logarithms of (p_T/m_Q) , through the evolution of FFs between the hard-scattering scale and the hadronization scale. In particular, the FF evolution with factorization scale is computed perturbatively, whereas a functional form for the FFs is fixed at a starting scale, including parameters fitted to experimental data obtained at leptonic colliders.

In the attempt of combining the best features of the two approaches, suitable for describing the heavy-meson production processes in different kinematical regimes, general-mass variable-flavour-number schemes have been proposed, which properly combine elements of the FFNS and the ZM-VFNS calculations. The recipe for this combination is not unique, with different GM-

VFNS implementations which differ for the way they handle it, which introduces an element of arbitrary. Among the most popular examples, we mention the FONLL [4] and the GM-VFNS [5, 6] approaches.

The issue with these approaches is that the limit for $m_Q \rightarrow 0$ of the FFNS calculation does not coincide with the result of the ZM-VFNS calculation. Subtraction terms are then introduced: $d\sigma^{sub} = \lim_{m \rightarrow 0} d\sigma^{FFNS} - d\sigma^{ZM-VFNS}$, such that the cross-section in a GM-VFNS scheme can be written as $d\sigma^{GM-VFNS} = d\sigma^{FFNS} - a d\sigma^{sub}$. The choice of the a term is scheme dependent. In particular, in FONLL a is a function of p_T and m_Q , i.e. $a = a(p_T, m_Q)$. The functional form is chosen in such a way that at small p_T the ZM-VFNS contribution is suppressed and the FONLL reduces to the FFNS. In the practical implementation, a specific functional form is fixed, and the evaluation of an uncertainty related to its possible variation is neither discussed nor included in the predictions used for data analyses. On the other hand, in the GM-VFNS of Ref. [5], $a = 1$, corresponding to the simplified-ACOT (S-ACOT) scheme. At small p_T , the S-ACOT GM-VFNS does not automatically reduce to the FFNS (unless $p_T = 0$), due to the presence of divergent contributions from amplitudes with heavy-quark initial states in which the heavy quark is treated as massless. These contributions can be switched off by an ad-hoc choice of the factorization scale [7]. Considering that, for those VFNS PDFs where $\mu_Q = m_Q$, the PDF $_Q(\mu_F < m_Q) = 0$, and using a scale $\mu_F = \xi \sqrt{p_T^2 + m_Q^2}$, the aforementioned contributions are switched off for $p_T < m_Q \sqrt{1/\xi^2 - 1}$. The value of ξ is chosen by comparing theoretical predictions with experimental data at small p_T . The renormalization scale can be chosen freely, whereas the factorization scale is fixed by the condition above. This is a limitation of this theoretical description. On the other hand, it has been shown that a rigorous factorization theorem applies even in this case, with the consequence that, similarly to what happens in the ZM-VFNS, the logarithms of p_T/m_Q can be resummed through the evolution of appropriate FF. FF fits consistently obtained in the GM-VFNS exist since long [8]. In general, for different GM-VFNS frameworks, different FF fits are required.

3. Comparisons of theory predictions with experimental data on the production of D mesons in pp collisions

In Fig. 1 we compare theory predictions obtained by different approaches to the experimental data of the ALICE collaboration for prompt D^+ and D^0 hadroproduction at $\sqrt{s} = 2.76$ TeV [9]. In all theory computations, we use as central renormalization scale $\mu_R = \mu_0 = \sqrt{p_T^2 + 4m_c^2}$. We use a factorization scale $\mu_F = \mu_0$, except for the GM-VFNS case, where we fix $\mu_F = \mu_0/2$ (see Section 2). The GM-VFNS prediction is shown together with its μ_R theory uncertainty band, arising from the variation $\mu_R \in [1/2, 2]\mu_0$. Additionally, central predictions obtained through the FFNS approach complemented by a phenomenological FF and those obtained by matching a NLO QCD computation of $c\bar{c}$ hadroproduction in the fixed-flavour-number-scheme with massive charm, with the parton shower (PS) + hadronization algorithms of the PYTHIA8 event generator [10], according to the POWHEG NLO+PS matching method [11, 12], are shown. For large p_T , the central GM-VFNS predictions turn out to be lower than the central NLO + PS ones, which lie on the upper edge of the GM-VFNS scale uncertainty band. Part of the differences are due to the different logarithmic accuracy of the two procedures, another part is related to the differences between the

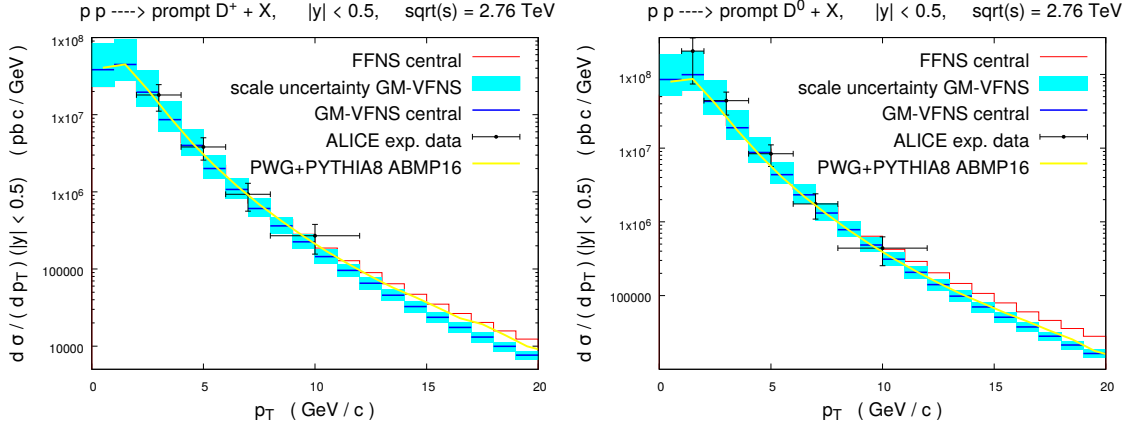


Figure 1: Theory predictions for the p_T distribution of prompt D^+ (left panel) and D^0 (right panel) hadroproduction vs. the ALICE experimental data at $\sqrt{s} = 2.76$ TeV of Ref. [9]. See the text for more detail.

non-perturbative parameters of the fragmentation functions/hadronization. FFNS NLO QCD predictions turn out to be much larger, due to the lack of resummation of logarithms of p_T/m_c . At small p_T , the three approaches give compatible predictions. When comparing to the experimental data for D^0 production, it is evident that for $p_T \sim 2 - 3$ GeV the three approaches produce central predictions which are smaller than the experimental data, although one can still conclude that there is full compatibility, when considering the theoretical and experimental uncertainty bands. At small p_T , the level of agreement between central theory predictions and experimental data turns out to be slightly larger for D^+ than for D^0 .

We observe a similar behaviour when comparing theory predictions with NLO QCD + PS accuracy with experimental data from LHCb collaboration, as shown in Fig. 2, where the pulls for data on open D^\pm production at 5 and 7 TeV are shown. The ratio between theory predictions and experimental data minus one is shown as a function of the p_T of the produced D^\pm meson. The ABMP16 PDFs [13] are used as an input for the calculation, and the band shown just refers to their uncertainty, computed from all available eigenvectors. Different panels refer to different rapidity bins. In particular, we observe that for some of the $(\sqrt{s}, \text{rapidity bin})$ combinations, the experimental data are 20 - 30 % larger than the central theory predictions for $p_T \sim 3 - 4$ GeV, with a noticeable shape difference. However, this does not apply to all combinations. This points to some inconsistency between D^\pm data at different \sqrt{s} . On the other hand, the fact that, for fixed \sqrt{s} , a similar discrepancy is observed for different rapidity bins, points to the fact that the discrepancies can not be all reabsorbed by a modification of the x dependence of the adopted PDFs, considering that different rapidity bins probe PDFs at different longitudinal momentum fractions x .

As a matter of fact, besides more precise PDF fits, other elements could contribute to increase the agreement between theory predictions and experimental data, which may be worth investigating. First, it can be useful revising FF fits and parameters of the hadronization models. In general-purpose shower Monte Carlo event generators, the hadronization parameters are fixed by a multi-step tuning procedure, which in turn might depend on many details. It might be worth making an effort towards a simultaneous tuning of the heavy-quark and light-quark hadronization/FF

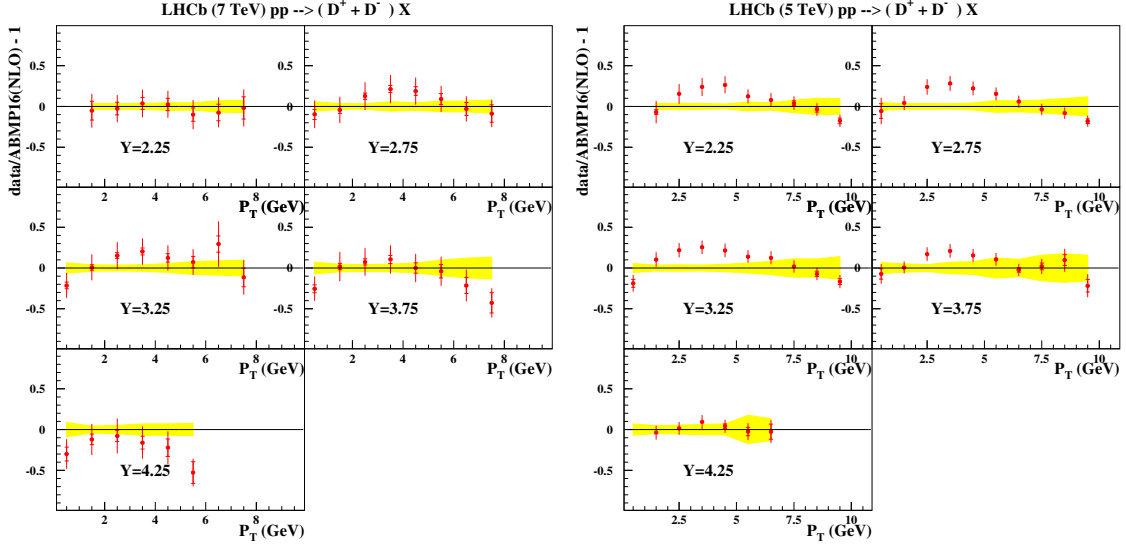


Figure 2: Pulls of the LHCb data for the p_T distributions of D^\pm in $pp \rightarrow D^\pm + X$ at a center-of-mass energy $\sqrt{s} = 7$ (left) and 5 (right) TeV, respectively. Each panel refers to a different rapidity bin. Theory predictions with NLO + PS accuracy are considered. Central predictions lie on the x axis. The solid band around the theoretical predictions is due to the uncertainties in the ABMP16 fit, used as input in this calculation. The μ_R and μ_F scale uncertainties are not shown and they would encompass the experimental data. See the text for more detail.

parameters using data on both light and heavy hadrons. Additionally, in case of the NLO + PS computations, a systematic retuning of the hadronization parameters could be necessary, as also advocated in Ref. [14], considering that their present values have been obtained by comparing to experimental data predictions from the standalone version of the Shower Monte Carlo codes, not including NLO corrections. Second, it can be useful including a reliable description of Multiple Parton Interactions: at present phenomenological models for MPI are implemented in general purpose Monte Carlo event generators. MPI parameters are also tuned. A retuning of the hadronization/FF parameters would have consequences even over the MPI parameters. The simplest case of MPI is Dual Parton Scattering, and considerable theoretical efforts have been performed to develop rigorous descriptions of the latter [15, 16], beyond the phenomenological pocket formula often used; it might be interesting to bridge the gap by applying more rigorous procedures to estimate the DPS contribution in the phenomenological analyses of heavy-flavour hadroproduction. Third, it is useful including higher-order corrections: the uncertainty band related to (μ_R, μ_F) scale variation, not shown in Fig. 2, is large, which points to the need of including higher-order corrections to reduce the theoretical uncertainties, that at present are much larger than the experimental ones. Fixed-order predictions including NNLO QCD corrections are already available for the total cross-sections for $Q\bar{Q}$ hadroproduction, for $Q = c, b, t$ [17, 18, 19, 20, 21]. Additionally, fixed-order predictions with NNLO QCD accuracy are already available for differential distributions for $t\bar{t}$ hadroproduction, using two different approaches [22, 23]. It is worth extending these computations to the case of lighter massive heavy quarks. In the q_T subtraction formalism [24], this might

require a careful monitoring of the behaviour of the cross-sections as a function of the parameter associated to the technical cut on q_T applied in the practical implementation. This parameter is introduced at intermediate steps to simplify the computation and then extrapolated to zero to get the cross-section. Additionally, resummation of different kinds of logarithms can modify the shape of the distributions and help to reduce the uncertainties. In particular, it is worth exploring the effects of threshold resummation (large x) in combination with the resummation of BFKL logarithms (small x). Fourth, it is useful improving the treatment of heavy-quark production and of the emissions from heavy quarks in Parton Shower algorithms. Among other things, this might require to explore multiple alternative solutions for the argument of α_S in the $g \rightarrow Q\bar{Q}$ splittings.

4. Implications for PDF fits

Improving the description of heavy-flavour production according to the aforementioned lines would have an impact on PDF fits, allowing for more precise gluon and sea quark PDF fits at small and large x values ($x < 10^{-4}$ and $x > 10^{-1}$).

In particular, several fits have already appeared in the literature, which include LHCb experimental data on open heavy-flavour production [25, 26]. In fact these data, which extend to very low p_T and large rapidities ($2 < y < 4.5$), allow to probe the low x region, $10^{-6} < x < 10^{-4}$. So far, ratios of data are typically used in the fits (i.e. ratios of rapidity distributions in different rapidity bins or ratio of data at different \sqrt{s}), due to the fact that in the ratios the huge scale uncertainty affecting the theory predictions greatly reduces. If an improved description of the p_T distributions will be obtained, then absolute differential cross-sections in p_T , besides rapidity distributions for each fixed p_T bin, could be used for fitting the PDF parameters. If predictions with a reduced scale uncertainty band become available, then PDF fits using absolute data (instead of ratios) can be performed with reduced uncertainty and improved constraints on the heavy-quark masses too, whose values can also be fitted together with the PDF parameters [27].

5. Comparisons between theory predictions and experimental data on the production of D mesons in pA collisions

Data on inclusive D meson production in pA collisions have also been released. Among others, the LHCb collaboration has employed very light targets (He) in a fixed-target configuration, collecting data on $p + \text{He}$ collisions at $\sqrt{s_{NN}} = 86.6$ GeV. This allows to study the relevance of cold nuclear matter effects for light nuclei. The comparison between their experimental data of Ref. [28] and theoretical predictions for the p_T and center-of-mass y distributions of D^0 mesons is shown in Fig. 3. The theoretical predictions, with NLO QCD + PS accuracy, refer to pp collisions. The effect of the He target is taken into account by superposition. The uncertainty band refers to scale variation. The total theoretical cross-sections after LHCb cuts amount to $\sigma(D^0 + \bar{D}^0) = 76.1 + 116$ (scale variation) - 35 (scale variation) $\mu\text{b/nucleon}$, in agreement with the experimental result $\sigma(D^0 + \bar{D}^0) = 80.8 \pm 2.4 \pm 6.3 \mu\text{b/nucleon}$. Notwithstanding the agreement within the uncertainty bands, at low p_T the central theoretical prediction for the p_T distribution has a slightly softer shape than the experimental data. Same applies for collisions with heavier nuclei. This points to the need of accounting for cold nuclear matter effects: in particular p_T broadening could enhance the

contributions at large p_T with respect to those at small p_T . A shape deformation is visible also in the rapidity distribution. Although theoretical predictions and experimental data agree when considering the uncertainty bands, the central theoretical predictions on the basis of the superposition approximation underestimate the experimental data at small absolute values of the rapidities. Including cold nuclear matter effects could enhance the theoretical predictions in this kinematical region, while decreasing those in the more backward rapidity bin. A careful study of this bin would be important to assess the role of intrinsic charm effects, which are supposed to enhance the contributions in this bin where large x PDFs ($x \in [0.17 - 0.37]$) are probed. At the moment the experimental data do not provide evidence for the existence of a significant intrinsic charm component, but theoretical predictions including cold nuclear matter effects should be considered before extracting firm conclusions on this. Considering the present difficulty in disentangling cold nuclear matter effects of different nature (initial state vs. final state effects), we believe that evidence for intrinsic charm should be searched for preferentially in pp collisions.

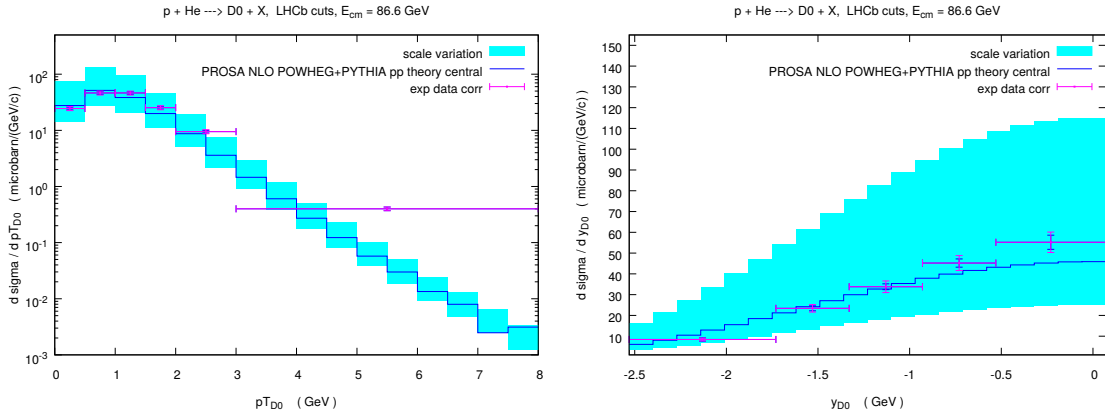


Figure 3: Transverse momentum and center-of-mass rapidity distributions for the D^0 mesons obtained in $p + \text{He} \rightarrow D^0 + X$ at $\sqrt{s_{NN}} = 86.6$ GeV, for the LHCb configuration of Ref. [28]. Experimental data are compared with theoretical predictions with NLO+PS accuracy, obtained using as input the PROSA 2015 PDFs [25]. In the theory predictions nuclear effects are approximated by the superposition model.

6. Implications for atmospheric charm

Improving the accuracy of the theoretical predictions for inclusive D -meson production in pA collisions might have an important impact on reducing the uncertainties on atmospheric charm production. This is important because atmospheric charm is a source of neutrinos and charged leptons (prompt lepton fluxes) which act as a background in the searches of cosmic neutrinos, travelling to the Earth from far astrophysical sources. Present estimates for the uncertainties on the atmospheric charm production process include QCD scale uncertainties, charm mass uncertainties and PDF uncertainties [29]. Most of the groups providing these estimate have worked in the superposition approximation. On the other hand, the data on charm production in pA collisions can be very useful for constraining nuclear PDF fits at low and large x values, which are an important input for these

calculations, and for better understanding the role of other cold nuclear matter effects, when nuclei of size similar to the most abundant air nuclei (N and O) are involved. The fixed-target data by LHCb are very useful for this kind of study. Further constraints on the intrinsic charm contribution would also be welcome, considering its possible effect on prompt neutrino fluxes [30].

7. Summary and conclusions

Starting from exemplificative comparisons with recent experimental data at the LHC, we have presented some open issues in the theoretical description of the single-inclusive production of heavy mesons, which might affect interesting applications like extraction of PDF and nPDF at small and large x values and estimates of the atmospheric prompt neutrino fluxes. Considering that the present experimental uncertainties on inclusive D -meson production in both pp and pA collisions are much smaller than the theoretical uncertainties, more accurate theoretical studies are welcome, acting on different elements, from the inclusion of higher-order corrections in the hard-scattering computation, to a more accurate modelization of the (parton shower + hadronization)/fragmentation processes.

References

- [1] **Particle Data Group** Collaboration, M. Tanabashi et al., *Review of Particle Physics*, *Phys. Rev.* **D98** (2018), no. 3 030001.
- [2] S. J. Brodsky, P. Hoyer, C. Peterson, and N. Sakai, *The Intrinsic Charm of the Proton*, *Phys. Lett.* **93B** (1980) 451–455.
- [3] **The xFitter Developers Team** Collaboration, V. Bertone et al., *Impact of the heavy quark matching scales in PDF fits*, *Eur. Phys. J.* **C77** (2017), no. 12 837, [[arXiv:1707.05343](#)].
- [4] M. Cacciari, M. Greco, and P. Nason, *The $P(T)$ spectrum in heavy flavor hadroproduction*, *JHEP* **05** (1998) 007, [[hep-ph/9803400](#)].
- [5] B. A. Kniehl, G. Kramer, I. Schienbein, and H. Spiesberger, *Inclusive D^{*+} production in p anti- p collisions with massive charm quarks*, *Phys. Rev.* **D71** (2005) 014018, [[hep-ph/0410289](#)].
- [6] M. Benzke, M. V. Garzelli, B. Kniehl, G. Kramer, S. Moch, and G. Sigl, *Prompt neutrinos from atmospheric charm in the general-mass variable-flavor-number scheme*, *JHEP* **12** (2017) 021, [[arXiv:1705.10386](#)].
- [7] B. A. Kniehl, G. Kramer, I. Schienbein, and H. Spiesberger, *Inclusive B -meson production at small p_T in the general-mass variable-flavor-number scheme*, *Eur. Phys. J.* **C75** (2015), no. 3 140, [[arXiv:1502.01001](#)].
- [8] T. Kneesch, B. A. Kniehl, G. Kramer, and I. Schienbein, *Charmed-meson fragmentation functions with finite-mass corrections*, *Nucl. Phys.* **B799** (2008) 34–59, [[arXiv:0712.0481](#)].
- [9] **ALICE** Collaboration, B. Abelev et al., *Measurement of charm production at central rapidity in proton-proton collisions at $\sqrt{s} = 2.76$ TeV*, *JHEP* **07** (2012) 191, [[arXiv:1205.4007](#)].
- [10] T. Sjöstrand, S. Ask, J. R. Christiansen, R. Corke, N. Desai, P. Ilten, S. Mrenna, S. Prestel, C. O. Rasmussen, and P. Z. Skands, *An Introduction to PYTHIA 8.2*, *Comput. Phys. Commun.* **191** (2015) 159–177, [[arXiv:1410.3012](#)].

- [11] P. Nason, *A New method for combining NLO QCD with shower Monte Carlo algorithms*, *JHEP* **11** (2004) 040, [[hep-ph/0409146](#)].
- [12] S. Frixione, P. Nason, and G. Ridolfi, *A Positive-weight next-to-leading-order Monte Carlo for heavy flavour hadroproduction*, *JHEP* **09** (2007) 126, [[arXiv:0707.3088](#)].
- [13] S. Alekhin, J. Blümlein, and S. Moch, *NLO PDFs from the ABMP16 fit*, *Eur. Phys. J.* **C78** (2018), no. 6 477, [[arXiv:1803.07537](#)].
- [14] M. Cacciari, S. Frixione, N. Houdeau, M. L. Mangano, P. Nason, and G. Ridolfi, *Theoretical predictions for charm and bottom production at the LHC*, *JHEP* **10** (2012) 137, [[arXiv:1205.6344](#)].
- [15] M. Diehl and J. R. Gaunt, *Double parton scattering theory overview*, *Adv. Ser. Direct. High Energy Phys.* **29** (2018) 7–28, [[arXiv:1710.04408](#)].
- [16] B. Cabouat, J. R. Gaunt, and K. Ostrolenk, *A Monte-Carlo Simulation of Double Parton Scattering*, *JHEP* **11** (2019) 061, [[arXiv:1906.04669](#)].
- [17] M. Czakon and A. Mitov, *Top++: A Program for the Calculation of the Top-Pair Cross-Section at Hadron Colliders*, *Comput. Phys. Commun.* **185** (2014) 2930, [[arXiv:1112.5675](#)].
- [18] M. Aliev, H. Lacker, U. Langenfeld, S. Moch, P. Uwer, and M. Wiedermann, *HATHOR: HAdronic Top and Heavy quarks crOss section calculatoR*, *Comput. Phys. Commun.* **182** (2011) 1034–1046, [[arXiv:1007.1327](#)].
- [19] M. V. Garzelli, S. Moch, and G. Sigl, *Lepton fluxes from atmospheric charm revisited*, *JHEP* **10** (2015) 115, [[arXiv:1507.01570](#)].
- [20] A. Accardi et al., *A Critical Appraisal and Evaluation of Modern PDFs*, *Eur. Phys. J.* **C76** (2016), no. 8 471, [[arXiv:1603.08906](#)].
- [21] M. L. Mangano et al., *Physics at a 100 TeV pp Collider: Standard Model Processes*, *CERN Yellow Rep.* (2017), no. 3 1–254, [[arXiv:1607.01831](#)].
- [22] M. Czakon, D. Heymes, and A. Mitov, *High-precision differential predictions for top-quark pairs at the LHC*, *Phys. Rev. Lett.* **116** (2016), no. 8 082003, [[arXiv:1511.00549](#)].
- [23] S. Catani, S. Devoto, M. Grazzini, S. Kallweit, and J. Mazzitelli, *Top-quark pair production at the LHC: Fully differential QCD predictions at NNLO*, *JHEP* **07** (2019) 100, [[arXiv:1906.06535](#)].
- [24] R. Bonciani, S. Catani, M. Grazzini, H. Sargsyan, and A. Torre, *The q_T subtraction method for top quark production at hadron colliders*, *Eur. Phys. J.* **C75** (2015), no. 12 581, [[arXiv:1508.03585](#)].
- [25] **PROSA** Collaboration, O. Zenaiev et al., *Impact of heavy-flavour production cross sections measured by the LHCb experiment on parton distribution functions at low x* , *Eur. Phys. J.* **C75** (2015), no. 8 396, [[arXiv:1503.04581](#)].
- [26] V. Bertone, R. Gauld, and J. Rojo, *Neutrino Telescopes as QCD Microscopes*, *JHEP* **01** (2019) 217, [[arXiv:1808.02034](#)].
- [27] **PROSA** Collaboration, O. Zenaiev, M. V. Garzelli, K. Lipka, S. O. Moch, A. Cooper-Sarkar, F. Olness, A. Geiser, and G. Sigl, *Improved constraints on parton distributions using LHCb, ALICE and HERA heavy-flavour measurements and implications for the predictions for prompt atmospheric-neutrino fluxes*, [arXiv:1911.13164](#).
- [28] **LHCb** Collaboration, R. Aaij et al., *First Measurement of Charm Production in its Fixed-Target Configuration at the LHC*, *Phys. Rev. Lett.* **122** (2019), no. 13 132002, [[arXiv:1810.07907](#)].

- [29] **PROSA** Collaboration, M. V. Garzelli, S. Moch, O. Zenaiev, A. Cooper-Sarkar, A. Geiser, K. Lipka, R. Placakyte, and G. Sigl, *Prompt neutrino fluxes in the atmosphere with PROSA parton distribution functions*, *JHEP* **05** (2017) 004, [[arXiv:1611.03815](#)].
- [30] R. Laha and S. J. Brodsky, *IceCube can constrain the intrinsic charm of the proton*, *Phys. Rev.* **D96** (2017), no. 12 123002, [[arXiv:1607.08240](#)].